Quantized spin waves in ferromagnetic and antiferromagnetic structures with domain walls

R. Wieser, E. Y. Vedmedenko, and R. Wiesendanger
Institut für Angewandte Physik und Zentrum für Mikrostrukturforschung, Universität Hamburg, Jungiusstrasse 11, D-20355 Hamburg, Germany

(Received 22 December 2008; revised manuscript received 11 February 2009; published 13 April 2009)

Quantized spin-wave modes in ferromagnetic and antiferromagnetic spin systems with transverse domain wall have been studied theoretically. We demonstrate that the analytical solutions for spin waves in systems with domain walls as well as for spin-wave patterns bound in the wall are in good agreement with numerical solutions found by means of Landau-Lifshitz-Gilbert dynamics. We discuss the difference between ferromagnetic and antiferromagnetic standing spin waves and explore standing spin waves in antiferromagnetic spin ring structures.

DOI: 10.1103/PhysRevB.79.144412 PACS number(s): 75.10.Hk, 75.40.Mg, 75.60.Ch

I. INTRODUCTION

At the beginning of magnetic data storage it was important to understand spin-wave excitations to minimize their disturbing influence or their assistance for the magnetization reversal.[1–3] More recent publications have shown that it is possible to use spin waves for logic devices.[4–6] Another route for logic and data storage applications is based on the use of magnetic domain walls (DWs).[7] At the moment both concepts seem to be far away from practical applications. Nevertheless we propose to combine the advantages of these two directions. To make a first step towards future devices using a combination of spin waves and domain walls the interaction between domain walls and spin waves has to be understood. In a previous publication we have shown that spin waves can be responsible for domain-wall motion and can influence the speed of moving domain walls.[8] In this paper we focus our attention on standing spin waves in confined systems with a domain wall at an atomic length scale. Contemporary logic devices and data storage have mesoscopic dimensions,[9] but in the future such devices might be realized on a much smaller length scale where not only ferromagnetic,[10,11] but also antiferromagnetic[12,13] and more complex spin structures[14–16] are important. To study spin waves in those nanosystems we use a classical Heisenberg model. This representation is a good approximation to describe itinerant magnets with a ferromagnetic, antiferromagnetic, or complex spin structure on the atomic length scale.[15] In this paper we restrict our investigations to ferromagnetic and antiferromagnetic one- and two-dimensional spin structures. This limitation should account for recent developments in fields of atomic manipulation and excitations.[17–19]

The paper is organized as follows. After introduction of the utilized model (Sec. II) the analytical calculations of spin waves in presence of a 180° transverse domain wall are described (Sec. II A) with solutions we need for comparison to the numerical calculations (Sec. III B). In Sec. III we describe spin waves in one-dimensional (Sec. III A) and two-dimensional (Sec. III B) ferromagnetic spin systems with a domain wall. In Sec. IV antiferromagnetic standing spin waves in the presence of a transverse domain wall (Sec. IV A) and standing spin waves in antiferromagnetic spin rings (Sec. IV B) will be investigated. Eventually a short summary is given (Sec. V).

II. MODEL

The model we consider is a classical Heisenberg spin model with energy contributions from the exchange interaction and the magnetic anisotropy. As has been recently shown[10,18,20] the simple Heisenberg model with uniaxial anisotropy is well suited for the description of magnetic nanostructures. Such a spin model is on the one hand the classical limit of a quantum mechanical, localized spin model; on the other hand it might be interpreted as a rigid sphere approximation (RSA) of an itinerant magnet.[21] Here, we focus our attention on the second interpretation. The magnetic properties are well described by the model Hamiltonian

$$\mathcal{H} = -J\sum_{\langle ij\rangle} \mathbf{S}_i \cdot \mathbf{S}_j - D_z\sum_i (S_i^z)^2, \tag{1}$$

where $\mathbf{S}_i = \boldsymbol{\mu}_i/\mu_s$ is a three-dimensional magnetic moment of unit length on a simple-cubic lattice with lattice constant a. The magnetic moment μ_s is given by $\mu_s = M_s a^3$, with the saturation magnetization M_s. The first sum in Eq. (1) is the exchange coupling between nearest neighbors with the coupling constant J. If $J>0$ the coupling is ferromagnetic. In this case all magnetic moments have a parallel alignment. If $J<0$ we have an antiferromagnetic coupling. In this case the system prefers an antiparallel orientation of the magnetic moments. The second sum represents a uniaxial anisotropy, favoring the z direction as the easy axis of the system ($D_z>0$).

In the following we present results for spin-wave excitations in one- and two-dimensional systems with a 180° transverse domain wall. Such systems can be understood as prototypes of atomic chains or stripes in the one-dimensional case and small islands in the two-dimensional case. The chains or stripes are parallel to the x axis. The domain wall is located in the middle of the system. In the domains the spins are oriented in $\pm z$ direction and inside the domain wall in y direction. The profile of the transverse domain wall is given by

$$S_y = \mathrm{sech}(x/\delta), \tag{2a}$$

$$S_z = -\tanh(x/\delta), \tag{2b}$$

where δ is the domain-wall width $\delta = \sqrt{Ja^2/2D_z}$.

In the two-dimensional case the domain wall is oriented parallel to the y axis. This means that the normal vector is oriented in $\pm x$ direction. The calculations were performed for fixed boundary conditions.

The underlying equation of motion for magnetic moments which we consider is the Landau-Lifshitz-Gilbert (LLG) equation

$$\frac{\partial \mathbf{S}_i}{\partial t} = -\frac{\gamma}{(1+\alpha^2)\mu_s}\mathbf{S}_i \times [\mathbf{H}_i + \alpha(\mathbf{S}_i \times \mathbf{H}_i)], \tag{3}$$

with the gyromagnetic ratio γ, the dimensionless Gilbert damping α, and the internal field $\mathbf{H}_i = -\partial \mathcal{H}/\partial \mathbf{S}_i$.

Solving of this equation leads to the time dependence of the magnetization and, hence, the spin-wave excitations we are interested in. On the one hand the Landau-Lifshitz-Gilbert equation can be solved analytically in the framework of micromagnetic theory. This gives a good understanding of the physics but we are restricted to some approximations. On the other hand the Landau-Lifshitz-Gilbert equation can be solved numerically. In the following we present both the analytical description as well as the numerical simulations of standing spin waves in the presence of a transverse domain wall.

A. Analytical calculation

Starting point of the analytical calculations is the Landau-Lifshitz-Gilbert equation (Eq. (3)) written in spherical coordinates

$$\mathbf{S} = \begin{pmatrix} S_x \\ S_y \\ S_z \end{pmatrix} = \begin{pmatrix} \sin\theta\cos\phi \\ \sin\theta\sin\phi \\ \cos\theta \end{pmatrix} \tag{4}$$

for vanishing damping $\alpha = 0$,

$$\frac{\partial \theta}{\partial t} = -\frac{\gamma}{M_s \sin\theta}\frac{\delta \mathcal{E}}{\delta \phi}, \tag{5a}$$

$$\frac{\partial \phi}{\partial t} = \frac{\gamma}{M_s \sin\theta}\frac{\delta \mathcal{E}}{\delta \theta}. \tag{5b}$$

The energy density $\mathcal{E}$, which is identical to $\mathcal{H}$ [Eq. (1)] in the continuum limit, is given by

$$\mathcal{E} = \int_{-\infty}^{+\infty} \left\{ A\left[\left(\frac{\partial\theta}{\partial x}\right)^2 + \sin^2\theta\left(\frac{\partial\phi}{\partial x}\right)^2\right] - K\cos^2\theta + C\sin^2\theta\cos^2\phi \right\} dx, \tag{6}$$

where $A = J/2a$ is the exchange stiffness, $K = D_z/a^3$ the easy axis anisotropy density, a the lattice constant, and M_s the saturation magnetization. To perform the analytical calculation we have to take into account a hard axis anisotropy $C \gg K$ along the x axis. Then we can follow Mikeska[22,23] and map Eq. (5) to the Sine-Gordon equation

$$\frac{\partial^2 \psi}{\partial t^2} - c_0^2\frac{\partial^2 \psi}{\partial x^2} + \omega_0^2 \sin\psi = 0, \tag{7}$$

with $\psi = 2\theta$, $c_0 = \sqrt{2\gamma^2 CA/M_s^2}$, and $\omega_0 = \sqrt{2\gamma^2 CK/M_s^2}$. One solution of this equation is the kink or antikink soliton

$$\psi = 4\arctan[\exp(\pm x/\delta)], \tag{8}$$

with $\delta = c_0/\omega_0 = \sqrt{A/K} = \sqrt{Ja^2/2D_z}$. These solutions are identical to the domain-wall profile of Eq. (2b),

$$\cos(\theta) = \cos(\psi/2) = \pm\tanh(x/\delta). \tag{9}$$

Now, we are interested in spin waves in the presence of a transverse domain wall. This means we have to search for solutions of the type

$$\Psi = \psi_s + \epsilon, \tag{10}$$

with ψ_s given by Eq. (8) and small fluctuations $|\epsilon| \ll 1$ around ψ_s. After introducing Ψ in the Sine-Gordon equation [Eq. (7)] and performing linearization with respect to ϵ we end up with the following equation:

$$\frac{\partial^2 \epsilon}{\partial t^2} - c_0^2\frac{\partial^2 \epsilon}{\partial x^2} + \omega_0^2\left[1 - 2\,\mathrm{sech}^2\left(\frac{x}{\delta}\right)\right]\epsilon = 0. \tag{11}$$

This equation can be solved using the following ansatz:

$$\epsilon(x,t) = f(x)e^{-i\omega t}, \tag{12}$$

which leads to the time-independent Schrödinger equation

$$\left(-\frac{\partial^2}{\partial x^2} + V(x)\right)f(x) = Ef(x), \tag{13}$$

with the Pöschel-Teller potential

$$V(x) = -\frac{2}{\delta^2}\mathrm{sech}^2\left(\frac{x}{\delta}\right) \tag{14}$$

and $E = (\omega^2 - \omega_0^2)/c_0^2$.

It is easy to show that this Schrödinger equation can be solved analytically.[24–26] We find two types of solutions. First, free spin-wave solutions are given by

$$f_e(x) = N\left[\cos(k_x x) - \tanh\left(\frac{x}{\delta}\right)\frac{\sin(k_x x)}{k_x\delta}\right], \tag{15a}$$

$$f_o(x) = N\left[k_x\delta\sin(k_x x) + \tanh\left(\frac{x}{\delta}\right)\cos(k_x x)\right], \tag{15b}$$

with $E = k_x^2$, which leads to the dispersion relation $\omega^2(k_x) = c_0^2 k_x^2 + \omega_0^2$. Here, c_0^2 is the spin-wave stiffness, ω_0^2 acts as an energy gap, and N is a normalization constant. Second, one spin-wave solution bound inside the domain wall is given by

$$f_b(x) = \mathrm{sech}\left(\frac{x}{\delta}\right), \tag{16}$$

with $E = -1/\delta^2 \Leftrightarrow \omega(k_x) = 0$. From soliton theory these solutions are well known. They represent a complete set of orthonormal functions.[27]

In the two-dimensional case[28,29] we have to replace the Laplacian $\partial^2/\partial x^2$ by $\partial^2/\partial x^2 + \partial^2/\partial y^2$ and the ansatz Eq. (12) by

$$\epsilon(x,y,t) = f(x)g(y)e^{-i\omega t}. \tag{17}$$

This leads to two separate differential equations for $f(x)$ and $g(y)$. Former is identical to Eq. (13) with $E=k_x^2=(\omega^2-\omega_0^2)/c_0^2-k_y^2 \Leftrightarrow \omega^2=c_0^2k^2+\omega_0^2$, with $k^2=k_x^2+k_y^2$ and $g(y)$ given by

$$\frac{\partial^2 g(y)}{\partial y^2} = -k_y^2 g(y). \tag{18}$$

For fixed boundary conditions the solution of this differential equation is

$$g(y) = \sin(k_y y). \tag{19}$$

B. Simulation

In this section a description of our simulation method will be given. So far the Hamilton function Eq. (1) describes the exchange interaction between the magnetic moments and the magnetic anisotropy due to the spin-orbit coupling only. Solving the Landau-Lifshitz-Gilbert equation Eq. (3) for such a Hamiltonian leads to a static configuration of magnetization. Here, we are interested in the dynamics of spin waves. This means that the magnetic moments have to be periodically excited. To do this we apply an oscillating external field, which is oriented in x direction perpendicular to the magnetic moments. Herewith the Hamilton function becomes

$$\mathcal{H} = \mathcal{H}_{\text{old}} - \mu_s B_{\text{OF}} \sum_i S_i^x \cos(\omega t), \tag{20}$$

with $\mathcal{H}_{\text{old}}$ given by Eq. (1). The second term describes the coupling to the external field $\mathbf{B}(t)=B_{\text{OF}}\cos(\omega t)\hat{\mathbf{x}}$ with oscillating frequency ω. Now the Landau-Lifshitz-Gilbert equation can be solved to get the time dependence of the magnetic moments $\mathbf{S}_i(t)$. To study standing spin waves we calculate the absorbed power P at each lattice point i as

$$P_i = -\left\langle \mu_s \left(\mathbf{S}_i \cdot \frac{d\mathbf{B}(t)}{dt} \right) \right\rangle = -\frac{\mu_s}{T}\int_0^T \mathbf{S}_i \cdot \frac{d\mathbf{B}}{dt} dt. \tag{21}$$

Physically P reflects the amount of energy (power) which is transformed into the spin-wave excitations.

The numerical procedure is as follows. The simulations start with a relaxed saturated magnetic structure for given J and D_z values where the magnetic moments are oriented in z direction. In the next step, an oscillating magnetic field is applied to all spins or one single spin and the absorbed power is calculated at each site over the time interval $\mathcal{T}$. P_i is positive when both $S_i^B(t)$ and $d\mathbf{B}(t)/dt$ have the same sign and negative for the case of opposite signs. The sign of P_i reflects the phase of the excitation at site i. The maximum (minimum) means an oscillation in phase (antiphase) with the time derivative of the oscillating field which corresponds to a phase shift of $+\pi/2$ $(-\pi/2)$ with respect to the oscillating field. $P_i=0$ means no or no arranged oscillation. The values of P_i can be immediately plotted as a function of the distance vector and thus yield spatially resolved spin-wave eigenmodes. The obtained patterns contain full information about the amplitude and the phase of an excitation. For larger time interval $\mathcal{T}$ the resolution of the normal modes is improved. To observe the absorbed power P as a function of frequency or an external field an averaging over the whole sample must be performed. The usual way of averaging is the integral response

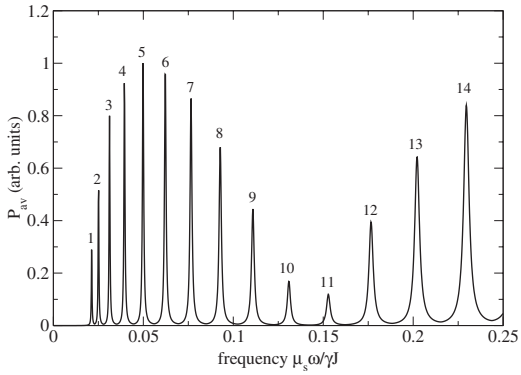

FIG. 1. Averaged absorbed power P_{av} as a function of frequency ω (single spin excitation) for a ferromagnetic chain with a transverse domain wall and two fixed ends. The numbers on top of the peaks correspond to the number of nodes n of the standing spin waves.

$$P_{\text{ir}} = \frac{1}{L}\sum_{i=1}^{L} P_i. \tag{22}$$

It is known, however, that the integral response signal P_{ir} does not show the whole spin-wave mode spectrum due to the fact that the spatial average over antisymmetric waves is zero. Therefore, the averaged resolved P_{av} signal has been introduced,

$$P_{\text{av}} = \frac{1}{L}\sum_{i=1}^{L} |P_i|. \tag{23}$$

With the help of Eq. (23) the power spectra, dispersion curves, and the field dependencies of normal modes can be easily calculated.

III. SPIN WAVES IN A FERROMAGNETIC SYSTEM WITH A DOMAIN WALL

In this section we describe the spin-wave excitation in the presence of a transverse domain wall in a ferromagnetic Heisenberg system. For the sake of simplicity we start with a one-dimensional ferromagnetic chain and then extend the calculations to two-dimensional systems.

A. Spin waves in one-dimensional chains with a domain wall

Figure 1 shows the averaged signal P_{av} as a function of frequency ω for a one-dimensional ferromagnetic chain with a transverse domain wall. The profile of the domain wall is given by Eq. (2), with $D_z/J=0.01$, and is also shown in Fig. 2(a). The peaks in Fig. 1 correspond to quantized standing spin-wave modes and the numbers given on top of each peak correspond to the serial number of nodes. The oscillation of

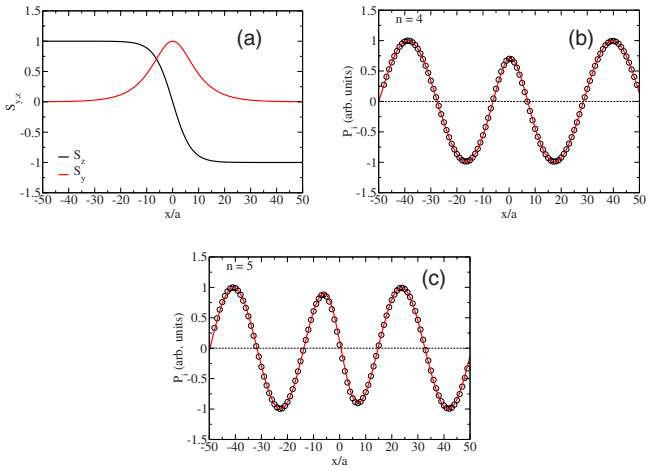

FIG. 2. (Color online) (a) Domain-wall profile and (b) even, and (c) odd standing spin-wave solutions of a linear ferromagnetic chain with a transverse domain wall. $D_z/J=0.01$ is assumed.

peak height corresponds to the type of excitation. In case of integral excitation (all spins are excited at the same time) the peak heights are nearly the same. In case of a point excitation a change in the peak heights occurs. This change depends on the relative position of the single point excitation and the position of the nodes. If the excitation is on top of a node the peak height is small. If the position coincides with a maximum or minimum, one gets a larger peak. As long as we are not interested in the peak height both methods lead to the same physical results. The shape of the standing spin waves can be also directly plotted. Figures 2(b) and 2(c) show two examples corresponding to an even and odd modes, respectively. The points are the numerical data and the solid line is the fitting curve which is given by the analytical solutions $f_e(x)$ [Eq. (15a)] and $f_o(x)$ [Eq. (15b)]. One can recognize a good agreement between the analytical curves in the case of an even-symmetry solution $f_e(x)$ as well as odd-symmetry solution $f_o(x)$ and the numerical data. Inside the domains the spin waves can be fitted by an ordinary sine or cosine function of constant amplitude and frequency. In the center of the domain wall the amplitude and frequency of the spin wave decrease. This behavior is well known and corresponds to a phase shift $\varphi=\arctan(\frac{1}{k_x\delta})$ of the spin waves passing through a domain wall.[4,30,31] In other words the phase decreases with increasing domain-wall width δ. At this point we have to stress that the function $\tanh(x/\delta)$ in Eq. (15) corresponds to the profile of the domain wall and has to be exchanged if the domain-wall profile changes.

In order to plot the dispersion relation one has to fit the analytical curves using the normalization factor N and the wave number k_x. The domain-wall width $\delta=\sqrt{Ja^2/2D_z}$ is uniquely defined via J and D_z. Taking the characteristic peak frequencies from Fig. 1 and the k_x values from the fitting procedure, the dispersion curve can be plotted and compared to the analytical dispersion

$$\hbar\omega \approx JSa^2k_x^2 + 2D_z. \tag{24}$$

Figure 3 shows the dispersion curve of a finite ferromagnetic chain (100 lattice sites) without (circle) and with a domain wall (square). One can see that both systems are well described by the same dispersion relation. Due to the presence of the domain wall the standing spin waves undergo a phase shift which can also be seen in the dispersion relation (Fig. 3) as a shift of the discrete energy levels.

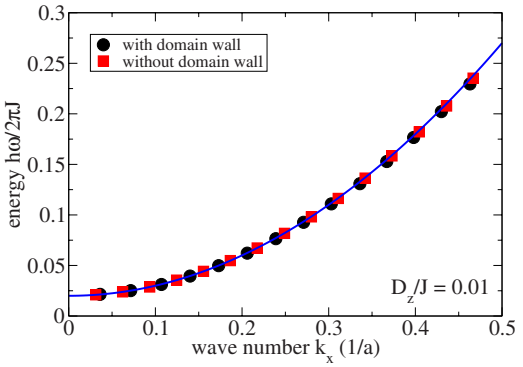

FIG. 3. (Color online) Dispersion relation of a ferromagnetic chain with transverse domain wall. The discrete points correspond to the standing spin-wave solutions in the presence or absence of a domain wall. The straight line represents the analytical dispersion curve given by Eq. (24).

B. Spin waves in two-dimensional systems with a domain wall

In this part of the paper we generalize the treatment of ferromagnetic spin waves in the presence of a transverse domain wall to two dimensions. This extension leads to some effects, which cannot be described in the limit of one-

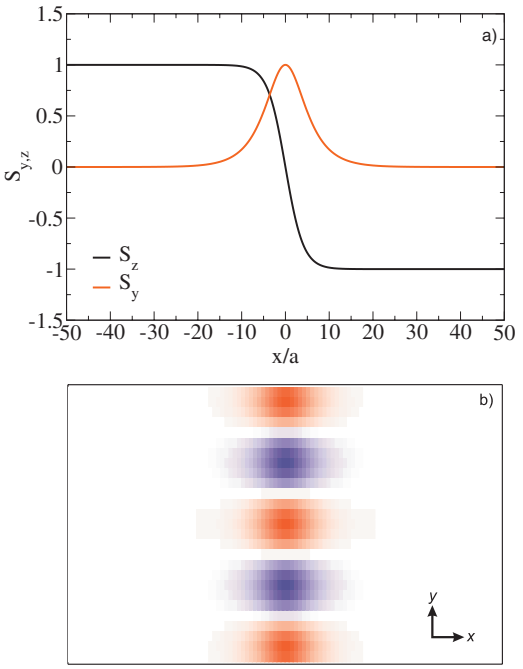

FIG. 4. (Color) (a) Domain-wall profile along the x axis of a two-dimensional ferromagnetic system and (b) top-view of the spatially resolved absorbed power $P_i(x,y)$. Different colors mark the maxima and minima of the absorbed power. White means no oscillation. $D_z/J=0.03$ is assumed.

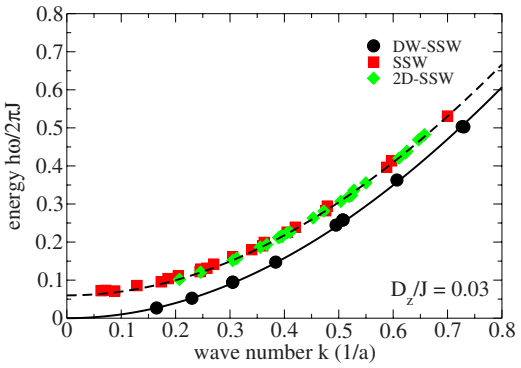

FIG. 5. (Color online) Dispersion relation of a two-dimensional ferromagnetic system. Due to the presence of a transverse domain wall two dispersion curves occur: one with an energy gap which corresponds to the free standing spin-wave solutions (SSW and 2D-SSW) and one without energy gap which corresponds to the bound spin modes (DW-SSW).

dimensional systems. Our numerical results show that in addition to the ordinary one-dimensional standing spin-wave solutions (SSWs) given by Eq. (15), additional superimposed solutions (2D-SSWs)

$$P(x,y) = f(x)\sin(k_y y) \tag{25}$$

can be found. Here, $f(x)$ is given by Eq. (15). The solutions of Eq. (25) result in additional peaks of the absorbed power. At last one can find spin-wave solutions bound inside the domain wall. Figure 4(a) shows the profile of the domain wall along the x axis while Fig. 4(b) gives the top view of the excitation map of the system. Different colors mark the minima and maxima of the spatially resolved absorbed power $P(x,y)$ whereas white areas mean no oscillation. The localization of the spin-wave mode as well as the additional nodes can be clearly seen in Fig. 4(b). The analytical solutions of these modes are given by

$$P(x,y) = \mathrm{sech}\left(\frac{x}{\delta}\right)\sin(k_y y). \tag{26}$$

The important point concerning these localized spin-wave modes is that due to the perpendicular orientation of the magnetization with respect to the anisotropy axis the anisotropy contribution to the energy inside the domain wall vanishes. This means that the energy dispersion of the bound excitations [DW-SSW, Eq. (26)] localized inside the domain wall has no energy gap,[28] in contrast to the one-dimensional [SSW, Eq. (15)] as well as to two-dimensional standing spin-wave modes [2D-SSW, Eq. (25)]. The dispersion relation of a two-dimensional system shown in Fig. 5 consists of two curves: one with an energy gap corresponding to SSW and 2D-SSW and the second one without a gap. This interesting property of the two-dimensional ferromagnetic system with domain wall might be used for new applications such as spin-wave logic. Furthermore such spin-wave modes strongly influence the electrical transport properties through the domain wall.[29]

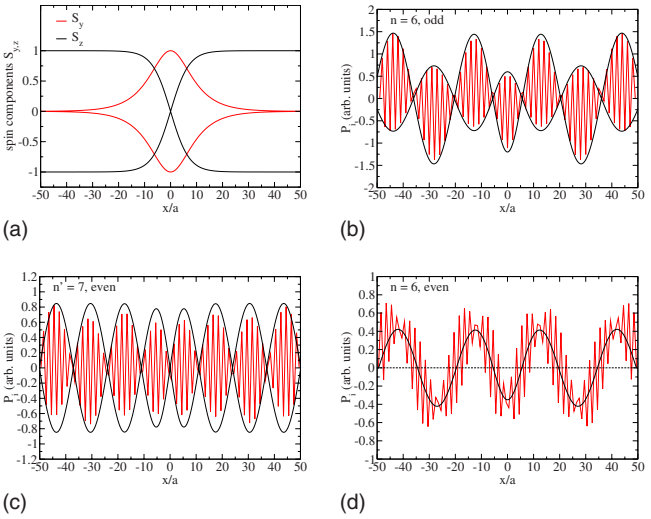

FIG. 6. (Color online) (a) Domain-wall profile and standing spin-wave modes in an antiferromagnetic spin chain with two fixed ends: (b) both ends belong to the same sublattice (odd number of lattice sites) or [(c) and (d)] to different sublattices (even number of atoms). $D_z/|J| = 0.01$ is assumed.

IV. SPIN WAVES IN ANTIFERROMAGNETIC DOMAIN-WALL SYSTEMS

The analytical calculation given in Sec. II A repeated for the case of an infinite antiferromagnet leads to the same solutions as before for each sublattice.[32] At first sight it seems that the antiferromagnetic solution consists of two sets of identical solutions as the two sublattices are degenerate. The only difference might lie in the two enveloping curves [see Fig. 6] of different sign due to the antiphase rotation of the magnetic moments in the two sublattices. Yet, careful analyses performed here and in the case of quantized antiferromagnetic spin waves in finite chains[33] show a completely different behavior in comparison to what one can expect from ferromagnetic spin waves. In the case of simple spin chains[33] the energetical degeneracy splits off and there is a strong influence of the boundary conditions as well as of the chain length.

In this section we proof the applicability of the derived analytical solutions to the case of antiferromagnetic chains with a transverse domain wall (Sec. IV A) and describe standing spin waves in antiferromagnetic ring structures (Sec. IV B).

A. Spin waves in antiferromagnetic chains with domain wall

The numerical procedure is the same as before in the case of a ferromagnet. We get similar discrete power spectra and shapes of spin waves. The profile of the domain wall is the same as before in the case of the ferromagnet. The only difference is that due to the antiparallel orientation of the two sublattices the relating formula Eq. (2) has been taken with different signs for both sublattices [see Fig. 6(a)]. In a previous publication,[33] we described several different boundary conditions. Here we limit our investigations to the mostly nontrivial case of an antiferromagnetic system with two fixed

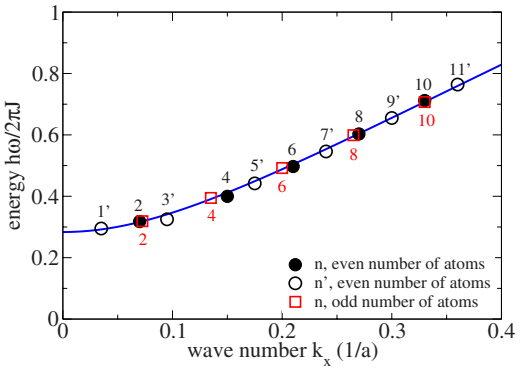

FIG. 7. (Color online) Dispersion curve of an antiferromagnetic Heisenberg chain with fixed ends and anisotropy $(D_z/|J|=0.01)$. Circles correspond to the two types of solutions of a chain with an even number of atoms and the squares correspond to the spin-wave modes of a chain with an odd number of lattice sites. Solid line represents the analytical solution given by Eq. (27).

ends. There are two variants of such a system. Either both ends belong to the same sublattice or to different sublattices. The difference between these two cases is just one magnetic moment but the effect on the spin waves of the antiferromagnetic chain is immense.[33] We expect similar behavior if a domain wall is introduced in such an antiferromagnetic one-dimensional structure. Here, we have investigated a chain of length L up to 99 lattice sites. In the first set of calculations both ends belonged to the same sublattice. Due to the existence of the domain wall the magnetic moments at the ends are oriented in opposite directions. According to our simulations such a system exhibits standing spin waves with an odd number of nodes only. The envelope can be fitted with the even solution Eq. (15a) but with different amplitudes for different sublattices [see Fig. 6(b)]. The wave number k_x is not affected by this asymmetry. The discrete energy values $\hbar\omega$ can be easily fitted by the well-known dispersion relation of an infinite antiferromagnetic chain,[33,34] [see Fig. 7]

$$\frac{\hbar\omega}{|J|} = \sqrt{4\sin^2(k_x a) + 2\frac{D_z}{|J|}\left(2\frac{D_z}{|J|} + 4\right)}. \tag{27}$$

The appearance of even spin-wave modes only can be understood on the basis of the fact that it is energetically more favorable if the nodes lie between two lattice points. If the number of nodes is odd the node in the middle will always coincide with one of the lattice points. That is why these spin-wave modes are excluded. For open boundary conditions we find two types of spin-wave modes with both even and odd numbers of nodes.[33] Due to the restriction of the boundary conditions only one solution out of four is found. The same arguments hold for the asymmetry of the standing spin waves. Joint action of the boundary conditions and the position of the nodes lead to the different number of positive and negative oscillations within one lobe of the enveloping curve. In other words the different number of the magnetic moments in the two sublattices (the difference is equal to one) leads to the different number of oscillations and hence to the asymmetric shape of the corresponding spin waves. Let us come to the second case, where both ends belong to different sublattices. The investigated chain length was taken to be up to 100 lattice sites. In this case the restriction of the boundary conditions is weaker and, therefore, it leads to the appearance of both even and odd spin-wave modes. Both types of modes can be fitted with the analytical solutions Eq. (15). The corresponding energy levels are well described by the dispersion relation of Eq. (27). While two enveloping curves of opposite signs Eq. (15b) exist in the case of an odd number of nodes the envelopes in the case of solutions Eq. (15a) have an identical sign but are shifted with respect to the initial curve. These two curves are visualized in Figs. 6(c) and 6(d) where the analytical solution without any displacement is also shown. Using the overall similarity with phonons we address these types of spin-wave modes as even acoustic and odd optical antiferromagnetic spin-wave modes.[33]

B. Spin waves in antiferromagnetic spin rings

So far we have explored antiferromagnetic chains. In this section antiferromagnetic spin rings will be investigated. Such a spin ring can be understood as a spin chain with periodic boundary conditions. The combination of periodic boundary conditions and an antiparallel alignment of the magnetic moments leads to the appearance of two cases depending on the chain length. If the number of lattice sites is even we end up with a nonfrustrated spin ring with the well-known Néel structure. For an odd number of lattice sites the antiferromagnetic structure is frustrated. Some of the nearest neighbors are oriented parallel to one another or in other words we find a domain wall.

In the following, we investigate antiferromagnetic spin systems without anisotropy $(D_z/|J|=0)$ to allow for a direct comparison to earlier quantum-mechanical calculations.[35] Let us start with the nonfrustrated spin ring (even number of lattice sites). The Néel structure is the ground-state configuration of such a spin ring even in the case of a pure quantum-mechanical system. In this case the expectation values of the magnetization component parallel to the quantization axis show a Néel structure. After the excitation of such a spin ring by an oscillating magnetic field as described above we find quantized spin waves with a simple cosine profile

$$P_m = \pm\cos(k_x x). \tag{28}$$

Due to the periodic boundary conditions an even number of nodes only [see Fig. 8(d)] may appear. At this point we expect the same behavior as in the case of the quantum-mechanical antiferromagnetic spin ring. The relaxation of a ring with an odd number of lattice sites leads to an antiferromagnetic spin structure with a domain wall. For absent anisotropy of the profile the domain wall is described by

$$S_y = \pm\cos\left(\frac{x\pi}{L}\right), \tag{29a}$$

$$S_z = \pm\sin\left(\frac{x\pi}{L}\right), \tag{29b}$$

with the domain-wall width δ given by the chain length L divided by π. Such magnetization configuration can be de-

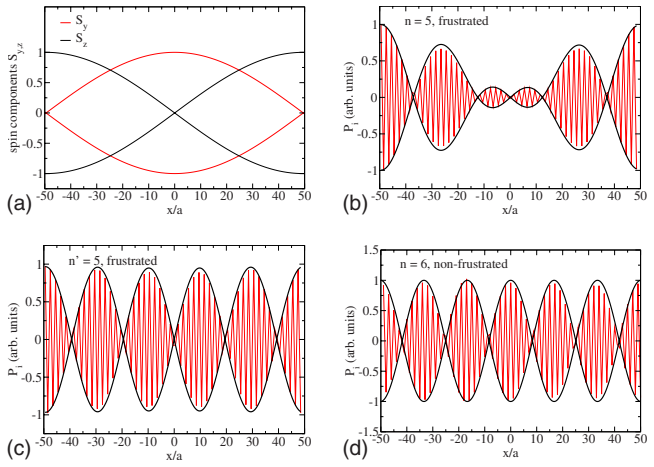

FIG. 8. (Color online) (a) Profile of the frustrated antiferromagnetic spin ring and [(b) and (c)] the corresponding types of standing spin waves. Plot (d) shows the standing spin-wave solution of the nonfrustrated antiferromagnetic spin ring. $(D_z/|J|=0)$ is assumed.

noted as a magnetic Möbius stripe because the ring should be rolled up twice to end up with the same orientation of the magnetization without abrupt changes. This means one has to follow the envelope curve (S_z component) of one sublattice first. After one round the sublattice has to be changed because of the periodic boundary conditions. After the second round the initial position of the lattice has been reached again.

Similarly to the antiferromagnetic spin chain we find in the second case (one lattice site more) two types of spin-wave solutions which are given by the following expressions:

$$P_n = \pm N\left[\cos(k_x x) - \frac{L}{k_x \pi}\sin\left(\frac{x\pi}{L}\right)\cos(k_x x)\right], \quad (30a)$$

$$P_{n'} = \pm N\left[\frac{k_x L}{\pi}\sin(k_x x) + \sin\left(\frac{x\pi}{L}\right)\cos(k_x x)\right], \quad (30b)$$

where n and n' denote the number of nodes. Because of the periodic boundary conditions only odd numbers of nodes exist. Furthermore, for each n mode a corresponding n' spin-wave mode with the same number of nodes has been found. The solution $P_{n'}$ can be understood as the equivalent to the odd solutions $f_o(x)$ of Eq. (15b) if we replace the domain-wall profile $S_z(x)=\tanh(x/\delta)$ [Eq. (2b)] by Eq. (29b) and the domain-wall width δ by L/π. The solution $f_e(x)$ [Eq. (15a)] has to be modified to admit the continuous symmetry of the ring. In order to get Eq. (30b) from Eq. (15a) one has to replace $\sin(k_x x)$ by $\cos(k_x x)$ and the prefactor $1/(k_x\delta)$ by δ/k_x. Additionally the domain-wall profile has to be replaced by Eq. (29b) and the domain-wall width by L/π. These equations can be used to fit the spin-wave structures with $n>1$ as well as $n'>1$ [see Figs. 8(b) and 8(c)] and to determine the quantized dispersion which is in good agreement with the analytical dispersion relation [Eq. (27)] of the infinite antiferromagnetic chain for zero anisotropy

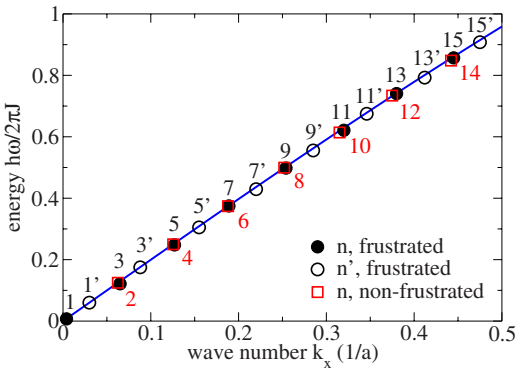

FIG. 9. (Color online) Dispersion relation of an antiferromagnetic spin ring. Symbols (circles and squares) correspond to the discrete standing spin-wave modes and the straight line gives the analytical solution Eq. (27) with $D_z/|J|=0$.

$$\frac{\hbar\omega}{|J|} = 2\,\sin(k_x a). \quad (31)$$

The same is true for the case of the nonfrustrated spin ring [see Fig. 9]. The special cases $n=n'=1$ with only one node are identical to the domain-wall profile which has been also seen in the case of the quantum-mechanical antiferromagnetic spin ring.[35]

V. SUMMARY

We have demonstrated that the spin waves in ferromagnetic as well as antiferromagnetic structures can be described by analytical solutions which are well known from theory of solitons. We have shown that the fitting of the numerical data by the analytical solutions taking into account the domain-wall profile leads to conventional ferromagnetic and antiferromagnets dispersion relations. In the case of two-dimensional ferromagnets we have confirmed numerically the existence of spin-wave modes bound inside the domain wall (DW-SSW). Such spin-wave modes have a gapless dispersion. We have demonstrated that the bound spin-wave modes can be excited independently. This is important for future applications.

In the second part of the paper we have explored antiferromagnetic spin waves. It has been demonstrated that the description of this kind of excitations is much more complicated because of a strong dependence of the spin-wave spectra on the number of lattice sites. The change of the chain length by one atom leads to a totally different behavior of the spin-wave modes. In the case of an antiferromagnetic chain with an odd number of lattice sites we find an asymmetric spin-wave mode with an even number of nodes only. This interesting behavior can be understood in the framework of the Peierls instability theory. In the case of an antiferromagnetic chain with an odd number of lattice sites two types of spin-wave modes have been found: even acoustic and odd optical antiferromagnetic spin-wave modes. Independently of the number of lattice sites (even or odd), the same analytical solutions can be used for the description of the shape of the spin waves as well as the dispersion curve.

In Sec. IV B, antiferromagnetic spin rings have been investigated. Similarly to the previous case different solutions have been found. If the number of lattice sites is even, the ground state is an ordinary Néel configuration. In this case only one type of spin-wave modes with an even number of nodes can be excited. In the case of an odd number of lattice sites a frustrated ground state has been found which leads to a magnetic Möbius-type ground state for $D_z/|J|=0$. In this case we find two types of odd spin-wave modes, which are well described by the analytical solution if the domain-wall profile is adjusted.

In conclusion, in all studied antiferromagnetic structures the presence of a transverse domain wall does not lead to a change of the dispersion curve; only the shape of the spin waves changes. The same is true for the ferromagnetic systems as well.

ACKNOWLEDGMENTS

Helpful discussions with N. Mikuszeit, A. Kubetzka, and K. von Bergmann are acknowledged. This work has been supported by the Deutsche Forschungsgemeinschaft in the framework of the subproject B3 of the SFB 668.

[1] C. Thirion, W. Wernsdorfer, and D. Mailly, Nature Mater. **2**, 524 (2003).
[2] H. T. Nembach, P. M. Pimentel, S. J. Hermsdoerfer, B. Leven, B. Hillebrands, and S. O. Demokritov, Appl. Phys. Lett. **90**, 062503 (2007).
[3] Z. Z. Sun and X. R. Wang, Phys. Rev. B **74**, 132401 (2006).
[4] R. Hertel, W. Wulfhekel, and J. Kirschner, Phys. Rev. Lett. **93**, 257202 (2004).
[5] T. Schneider, A. A. Serga, B. Leven, B. Hillebrands, R. L. Stamps, and M. P. Kostylev, Appl. Phys. Lett. **92**, 022505 (2008).
[6] A. Khitun, B. Mingqiang, and K. L. Wang, IEEE Trans. Magn. **44**, 2141 (2008).
[7] D. A. Allwood, G. Xiong, C. C. Faulkner, D. Atkinson, D. Petit, and R. P. Cowburn, Science **309**, 1688 (2005).
[8] R. Wieser, U. Nowak, and K. D. Usadel, Phys. Rev. B **69**, 064401 (2004).
[9] M. Hayashi, L. Thomas, R. Moriya, C. Rettner, and S. S. P. Parkin, Science **320**, 209 (2008).
[10] E. Y. Vedmedenko, A. Kubetzka, K. von Bergmann, O. Pietzsch, M. Bode, J. Kirschner, H. P. Oepen, and R. Wiesendanger, Phys. Rev. Lett. **92**, 077207 (2004).
[11] E. Y. Vedmedenko, K. von Bergmann, H. P. Oepen, and R. Wiesendanger, J. Magn. Magn. Mater. **290-291**, 746 (2005).
[12] A. Kubetzka, P. Ferriani, M. Bode, S. Heinze, G. Bihlmayer, K. von Bergmann, O. Pietzsch, S. Blügel, and R. Wiesendanger, Phys. Rev. Lett. **94**, 087204 (2005).
[13] M. Bode, E. Y. Vedmedenko, K. von Bergmann, A. Kubetzka, P. Ferriani, S. Heinze, and R. Wiesendanger, Nature Mater. **5**, 477 (2006).
[14] P. Kurz, G. Bihlmayer, K. Hirai, and S. Blügel, Phys. Rev. Lett. **86**, 1106 (2001).
[15] R. Wieser, E. Y. Vedmedenko, and R. Wiesendanger, Phys. Rev. B **77**, 064410 (2008).
[16] P. Ferriani, K. von Bergmann, E. Y. Vedmedenko, S. Heinze, M. Bode, M. Heide, G. Bihlmayer, S. Blügel, and R. Wiesendanger, Phys. Rev. Lett. **101**, 027201 (2008).
[17] C. F. Hirjibehedin, C. P. Lutz, and A. J. Heinrich, Science **312**, 1021 (2006).
[18] P. Gambardella, Nature Mater. **5**, 431 (2006).
[19] F. Meier, L. Zhou, J. Wiebe, and R. Wiesendanger, Science **320**, 82 (2008).
[20] U. Nowak, O. N. Mryasov, R. Wieser, K. Guslienko, and R. W. Chantrell, Phys. Rev. B **72**, 172410 (2005).
[21] V. P. Antropov, M. I. Katsnelson, B. N. Harmon, M. van Schilfgaarde, and D. Kusnezov, Phys. Rev. B **54**, 1019 (1996).
[22] H. J. Mikeska, J. Phys. C **11**, L29 (1978).
[23] H. J. Mikeska, J. Appl. Phys. **52**, 1950 (1981).
[24] S. Flügge, *Practical Quantum Mechanics* (Springer, Berlin, 1994).
[25] J. Lekner, Am. J. Phys. **75**, 1151 (2007).
[26] H. B. Braun, Phys. Rev. B **50**, 16485 (1994).
[27] T. Dauxois and M. Peyrard, *Physics of Solitons* (Cambridge University Press, Cambridge, England, 2006).
[28] A. V. Ferrer, P. F. Farinas, and A. O. Caldeira, Phys. Rev. Lett. **91**, 226803 (2003).
[29] A. V. Ferrer, P. F. Farinas, and A. O. Caldeira, Philos. Mag. **85**, 2293 (2005).
[30] R. K. Dodd, J. C. Eilbeck, J. D. Gibbon, and H. C. Morris, *Solitons and Nonlinear Wave Equations* (Academic, London, 1982).
[31] C. Bayer, H. Schultheiss, B. Hillebrands, and R. L. Stamps, IEEE Trans. Magn. **41**, 3094 (2005).
[32] D. I. Paul, Phys. Rev. **126**, 78 (1962).
[33] R. Wieser, E. Y. Vedmedenko, and R. Wiesendanger, Phys. Rev. Lett. **101**, 177202 (2008).
[34] F. Keffer and C. Kittel, Phys. Rev. **85**, 329 (1952).
[35] J. Schnack and P. Shchelokovskyy, J. Magn. Magn. Mater. **306**, 79 (2006).